

## Supporting Information

### Simultaneously Improving Efficiency, Stability and Intrinsic Stretchability of Organic Photovoltaic Films via Molecular Toughening

Kaihu Xian, Kai Zhang, Tao Zhang, Kangkang Zhou, Zhiguo Zhang, Jianhui Hou, Haoli Zhang, Yanhou Geng, and Long Ye\*

#### 1. Experimental Section

**Materials.** All chemicals were purchased from commercial sources without further purification unless otherwise noted. PH1000 and PEDOT:PSS (AI4083) was purchased from the CleviosTM. PM6 and eC9 were purchased from Solarmer Materials Inc and PNDIT-F3N were purchased from eFlexPV Limited. TDY- $\alpha$  was synthesized by Zhang's group according their previous work<sup>1</sup>. All solvents were purchased from Sigma Aldrich or Heowns.

**Device Fabrication.** The rigid device structure of ITO glass substrate/PEDOT:PSS/active layer/PNDIT-F3N/Ag was adopt in this study, while the intrinsically stretchable devices is on a TPU/modified PH1000 substrate with EGaIn cathode. The PH1000 was modified according previous report<sup>2</sup>. The blend systems with 100 nm thickness of active layers were dissolved in CF at the total concentration of 15 mg mL<sup>-1</sup>. In the study of green solvents, the blends with 100 nm active layer thickness were dissolved in THF at the total concentration of 15 mg mL<sup>-1</sup> and in Tol at the donor concentration of 6 mg mL<sup>-1</sup>. Moreover, the donor concentration of thick active layer in *o*-XY is 10 mg mL<sup>-1</sup> for 70, 100 nm; 15 mg mL<sup>-1</sup> for 150, 200 nm; 23 mg mL<sup>-1</sup> for 300, 500 nm; 30 mg mL<sup>-1</sup> for 700, 1000 nm. The CF/THF blend solutions were stirred at 50 °C for 4 h and the Tol/ *o*-XY blend solutions were stirred at 90 °C for 4 h to fully dissolve. The optimal D/A ratio was 1:1.2 (w/w) in all active layers, and the only difference is the TDY- $\alpha$  content in acceptors. Prior to spin-coating the active layer solutions, 0.5% DIO (v/v) was added into the solutions. PNDIT-F3N was dissolved in methanol at the concentration of 0.5 mg mL<sup>-1</sup> with 0.5% acetic acid. Devices were fabricated as follows. First, ITO substrates were treated with UV ozone for 25 min. Then, about 20 nm PEDOT:PSS layers were deposited via spin-coating on the pre-cleaned ITO substrates and annealed at 150 °C for 20 min. Subsequently, the substrates were transferred to the argon-filled glove box. The mixed solutions were spin-coated onto the PEDOT:PSS layers, Note that the blend films were treated with thermal annealing at 100 °C for 10 minutes. PNDIT-F3N was spin-coated on the top of the active layers. Finally,

100 nm thick Ag was deposited on the top of PNDIT-F3N layer under high vacuum. The fabrication process of intrinsically stretchable devices is exactly the same as that of rigid devices except that the top electrode is sprayed-coated with EGaIn (25 wt% In and 75 wt% Ga) in air. The effective area of the small area cells is about 0.04 cm<sup>2</sup>.

## 2. Instruments and Measurement

**Optical Absorption.** Absorption spectra of all the materials in the solid thin films were measured on Shimadzu UV3600 plus spectrometer. Thin-films were prepared by spin coating from the solutions.

**Photovoltaic Properties.** The *J-V* measurements were performed via the AAA solar simulator (SS-F5-3A, Enli Technology Co. Ltd, Taiwan) along with AM 1.5G spectra whose intensity was calibrated by the certified standard silicon solar cell at 100 mW cm<sup>-2</sup>. The EQE spectra were measured through the Solar Cell Spectral Response Measurement System QE-R3011 (Enli Technology Co. Ltd, Taiwan). The thickness of blend layers was measured via the surface profilometer Bruker Dektak XT.

**Charge Transport Properties.** The hole and electron mobilities were measured by the space charge limited current (SCLC) method, employing device architectures of ITO/PEDOT:PSS/active layer/MoO<sub>3</sub>/Ag and ITO/ZnO/active layer/PNDIT-F3N/Ag, respectively. The mobilities were obtained by taking the dark current-voltage curves in the range 0-7 V and fitting the results to a space charge limited form. The equation  $J = (9/8)\varepsilon_0\varepsilon\mu_0V^2/L^3 \exp[-(0.89\sqrt{V/E_0}L)]$  was used to calculate the hole mobilities. where  $J$  is the current density,  $\varepsilon_0$  is the vacuum permittivity,  $\varepsilon$  is the relative permittivity of the organic donor material,  $\mu$  is the charge carrier mobility,  $V$  is the effective applied voltage,  $L$  is the thickness of the film. And the equation  $J = (9/8)\varepsilon_0\varepsilon_r\mu_eV^2/L^3$  was used to calculate the electron mobilities, where  $\varepsilon_r$  is the relative permittivity of the organic acceptor material,  $\mu$  is the charge carrier mobility.

**Mechanical Measurements.** Stress-strain curves were acquired using a high-precision FOW instrument (Yangzhou Superior Flexible Optoelectronic Company, China). In the FOW test, the blend films were coated on precleaned glasses (size: 2 × 2 cm) and then cut into a rectangle shape and transferred to the water surface. The blend films were moved above the PDMS fixture and then glued to the PDMS by lowering the liquid level. FOE tests were carried out using a polarizing microscope (ECLIPSE LV100N POL, Nikon) and a custom-designed tensile stage.

The films were coated on glasses (size:  $1.7 \times 1.7$  cm) and then transferred to the PDMS film via water. The crack-onset strains of films were measured by stretching PDMS until the films started to crack under the observation of a polarized light microscope.

**Morphology Characterizations.** The surface morphology of films was measured by a Nanoscope V AFM (Bruker Multimode 8) in tapping mode. The scanning area was  $2 \mu\text{m} \times 2 \mu\text{m}$  and the scanning rate is set to 1 Hz for the resolution ( $256 \times 256$ ).

**GIWAXS Characterizations.** The samples for GIWAXS measurements were prepared on silicon substrates and the conditions were the same as the device preparation. GIWAXS experiments were carried out at BL02U2 beamline of Shanghai Synchrotron Radiation Facility (SSRF). The X-ray energy was 10 keV, corresponding to the wavelength of  $1.24 \text{ \AA}$ . The incidence angle was  $0.20^\circ$  and the sample-to-detector distance was 313 mm by careful calibration. The beam center and sample-to-detector distance were calibrated with LaB<sub>6</sub>.

**Surface Tension Characterization.** The surface tension of the films was calculated from deionized water ( $\text{H}_2\text{O}$ ) and ethylene glycol (EG) contact angle measurements of the films according to the Wu's model:

$$\gamma_{\text{water}}(1 + \cos\theta_{\text{water}}) = \frac{4\gamma_{\text{water}}^d\gamma^d}{\gamma_{\text{water}}^d + \gamma^d} + \frac{4\gamma_{\text{water}}^p\gamma^p}{\gamma_{\text{water}}^p + \gamma^p}$$

$$\gamma_{\text{EG}}(1 + \cos\theta_{\text{EG}}) = \frac{4\gamma_{\text{EG}}^d\gamma^d}{\gamma_{\text{EG}}^d + \gamma^d} + \frac{4\gamma_{\text{EG}}^p\gamma^p}{\gamma_{\text{EG}}^p + \gamma^p}$$

$$\gamma = \gamma^d + \gamma^p$$

where  $\theta$  refers to the contact angle of each film and  $\gamma$  is the surface tension of the materials, which is equal to the sum of the dispersion ( $\gamma^d$ ) and polarity ( $\gamma^p$ ) components;  $\gamma_{\text{water}}$  and  $\gamma_{\text{EG}}$  are the surface tensions of the water and ethylene glycol;  $\gamma_{\text{water}}^d$  and  $\gamma_{\text{water}}^p$ ,  $\gamma_{\text{EG}}^d$  and  $\gamma_{\text{EG}}^p$  are the dispersion and polarity components of  $\gamma_{\text{water}}$  and  $\gamma_{\text{EG}}$ , respectively.

**Miscibility Characterization.** The Flory-Huggins interaction parameters ( $\chi_{da}$ ) were calculated through surface energy,<sup>3</sup> according to the equation:

$$\chi_{da} = K(\sqrt{\gamma_d} - \sqrt{\gamma_a})^2$$

Where  $K$  is a constant, and  $\gamma$  is the surface tension of the materials.  $\gamma_d$  and  $\gamma_a$  refer to the surface tension of the polymer donor and small molecule acceptors, respectively.

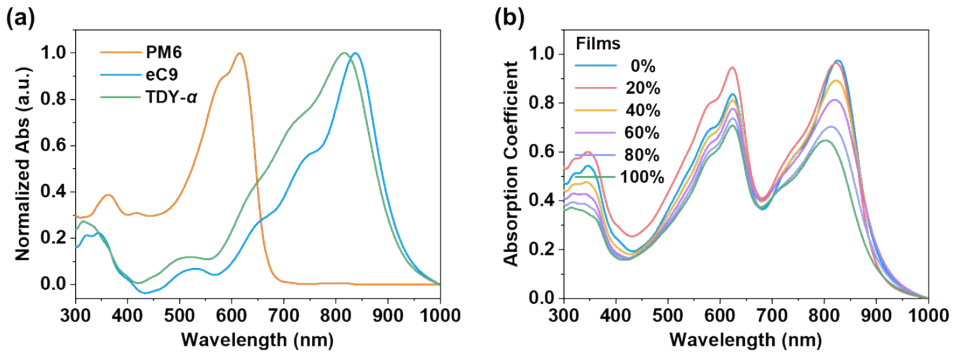


**Figure S1.** Normalized absorption spectra of PM6, eC9 and TDY- $\alpha$  neat films and their blend films with the change of the TDY- $\alpha$  ratio.

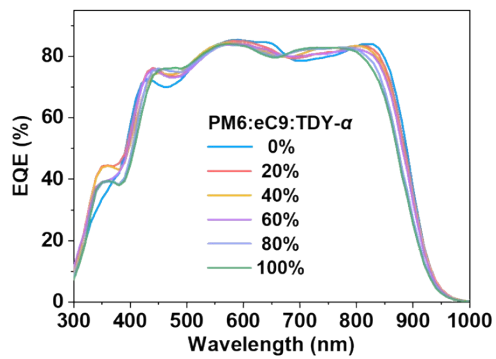


**Figure S2.** The EQE curves of relevant devices with different amounts of TDY- $\alpha$ .

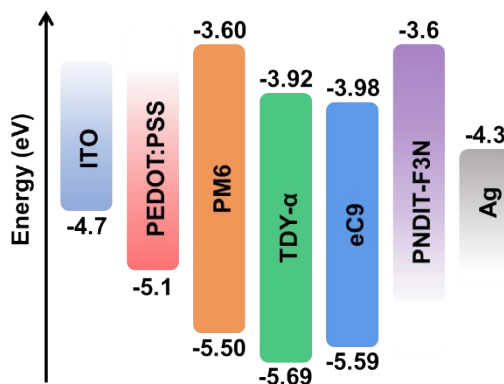


**Figure S3.** Energy level diagram of all the materials.

**Table S1.** Detailed  $EQE_{EL}$  and  $\Delta E_3$  values of the PM6:eC9:TDY- $\alpha$ -based OPV cells.

TDY- $\alpha$ (wt%)	0	20	40	60	80	100
$EQE_{EL}$	1.76E-4	2.00E-4	1.56E-4	1.51E-4	1.45E-4	0.95E-4
$\Delta E_3$ (eV)	0.224	0.220	0.227	0.228	0.229	0.240

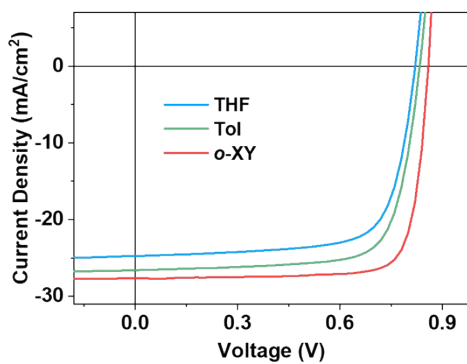


**Figure S4.**  $J$ - $V$  curves of the PM6:eC9:TDY- $\alpha$ -based optimized rigid devices in different solvents. ITO was used as the substrate. The film thickness is 100 nm.

**Table S2.** Detailed photovoltaic parameters of PM6:eC9:TDY- $\alpha$ -based OPV rigid devices in different solvents under the illumination of AM 1.5G. ITO was used as the substrate. The film thickness is 100 nm.

Solvent	$V_{OC}$ (V)	$J_{SC}$ ( $\text{mA cm}^{-2}$ )	FF (%)	PCE (%)
CF	0.855	27.23	80.73	18.80
THF	0.821	24.74	72.63	14.74
Tol	0.834	26.58	74.49	16.51
<i>o</i> -XY	0.856	27.62	80.77	19.10

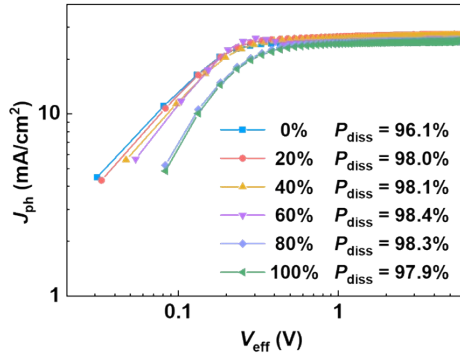


**Figure S5.**  $J_{ph}$  versus  $V_{eff}$  plots of all the blend devices.

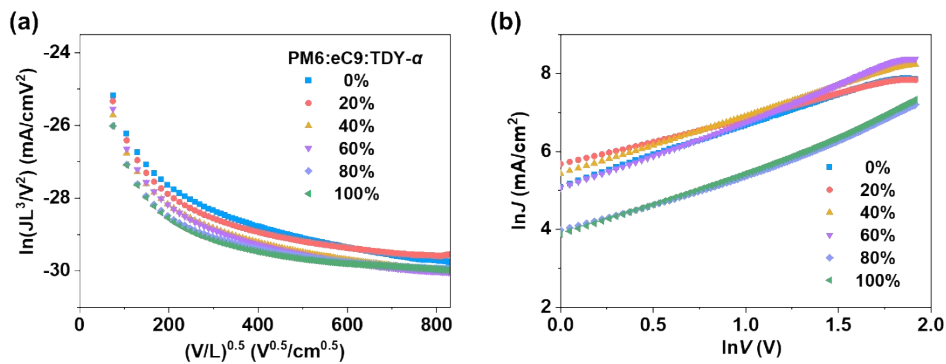


**Figure S6.** The (a) hole and (b) electron mobilities of all the blend films with different amounts of TDY- $\alpha$  measured by SCLC method.

**Table S3.** The detailed hole and electron mobilities parameters and  $\mu_h/\mu_e$  values.

TDY- $\alpha$ (wt%)	0	20	40	60	80	100
Hole ( $\text{cm}^2 \text{V}^{-1} \text{s}^{-1}$ )	0.0021	0.0012	0.0011	9.89E-04	7.86E-04	7.25E-04
Electron ( $\text{cm}^2 \text{V}^{-1} \text{s}^{-1}$ )	5.45E-04	9.79E-04	7.67E-04	5.34E-04	1.79E-04	1.62E-04
$\mu_h/\mu_e$	3.87	1.25	1.41	1.85	4.39	4.49

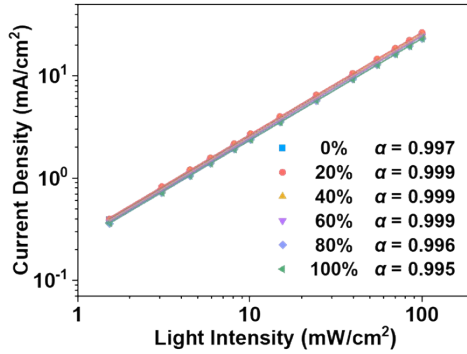


**Figure S7.** The extracted plots of  $J_{SC}$  versus light intensity for the devices.

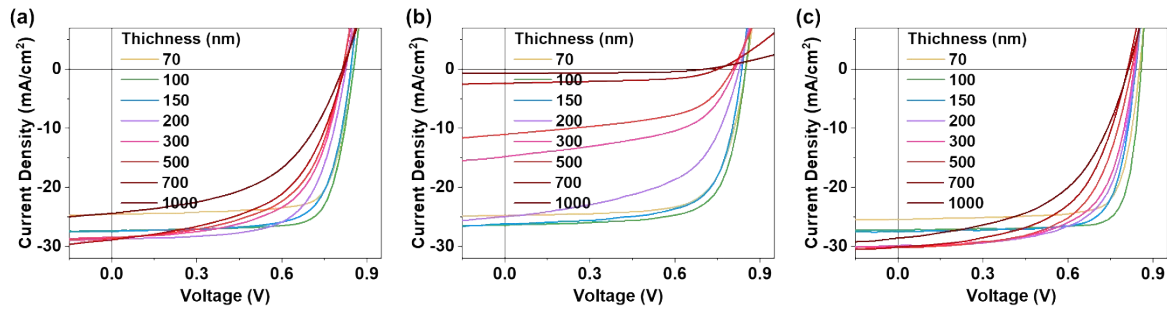


**Figure S8.**  $J$ - $V$  curves of (a) PM6:eC9, (b) PM6:TDY- $\alpha$  and (c) PM6:eC9:TDY- $\alpha$ -based optimized rigid devices with different thicknesses.

**Table S4.** Detailed photovoltaic parameters of PM6:eC9-based rigid devices with different thicknesses.

Thickness (nm)	$V_{OC}$ (V)	$J_{SC}$ ( $\text{mA cm}^{-2}$ )	FF (%)	PCE (%)
70	0.843	24.55	76.80	15.89
100	0.852	27.35	76.27	17.76
150	0.843	27.46	72.08	16.68
200	0.825	28.78	66.55	15.80
300	0.815	28.49	60.91	14.14
500	0.814	28.62	57.69	13.43
700	0.820	28.93	53.45	12.68
1000	0.814	24.42	51.10	10.15

**Table S5.** Detailed photovoltaic parameters of PM6:TDY- $\alpha$  blends with different thicknesses.

Thickness (nm)	$V_{OC}$ (V)	$J_{SC}$ (mA cm $^{-2}$ )	FF (%)	PCE (%)
70	0.850	24.77	70.65	14.87
100	0.848	26.41	71.55	16.02
150	0.834	26.22	68.63	14.97
200	0.826	24.97	54.64	11.24
300	0.810	14.81	52.20	6.25
500	0.803	11.05	52.30	4.62
700	0.752	2.40	52.63	0.95
1000	0.707	0.709	56.37	0.28

**Table S6.** Detailed photovoltaic parameters of PM6:eC9:TDY- $\alpha$ -based rigid devices with different thicknesses under the illumination of AM 1.5G.

Thickness (nm)	$V_{OC}$ (V)	$J_{SC}$ (mA cm $^{-2}$ )	FF (%)	PCE (%)
70	0.851	25.42	77.43	16.76
100	0.856	27.62	80.77	19.10
150	0.838	27.53	75.60	17.38
200	0.834	29.86	66.53	16.51
300	0.831	30.02	64.02	15.93
500	0.824	30.24	60.79	15.09
700	0.810	30.09	56.65	13.80
1000	0.813	28.61	51.92	12.08

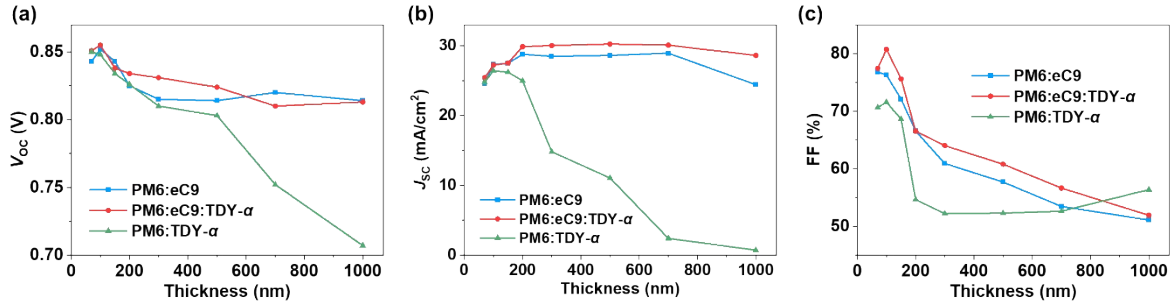


**Figure S9.** The evolution plots of (a)  $V_{oc}$ , (b)  $J_{sc}$ , and (c) FF of the two binary and optimal ternary rigid devices with different thicknesses.

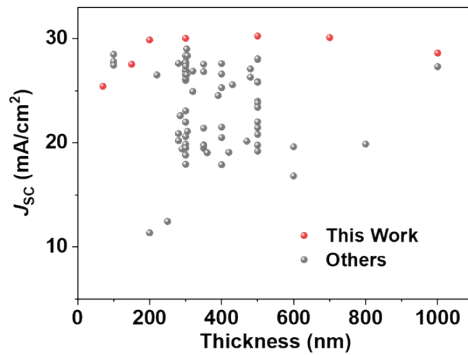


**Figure S10.** Plots of the  $J_{sc}$  as a function of active layer thickness for different systems.

**Table S7.** Summary of the recent representative thick-film OPVs.

Active layers	Thickness (nm)	$V_{oc}$ (V)	$J_{sc}$ (mA cm <sup>-2</sup> )	FF (%)	PCE (%)	Ref.
D18:eC9	100	0.886	28.48	79.79	20.12	<sup>4</sup>
PB2:BTP-eC9:FTCC-Br	100	0.891	27.8	81.5	20.2	<sup>5</sup>
D18-Cl:BTP-4F-P2EH	100	0.923	27.9	80.8	20.8	<sup>6</sup>
P3HT:IC <sub>60</sub> BA	200	0.870	11.35	75.00	7.40	<sup>7</sup>
D18:L8-BO	220	0.898	26.50	74.50	17.70	<sup>8</sup>
	300	0.897	27.80	67.80	16.90	

	400	0.892	27.60	66.30	16.30	
	500	0.886	28.00	64.90	16.00	
PBnDT-FTAZ:PC <sub>61</sub> BM	250	0.790	12.45	72.20	7.10	<sup>9</sup>
PNTT:BTR:PC <sub>71</sub> BM	280	0.750	20.88	70.67	11.44	<sup>10</sup>
PNTT:PC <sub>71</sub> BM	280	0.770	20.20	71.80	11.30	<sup>11</sup>
PM6:Y6:PP	280	0.830	27.61	67.00	15.47	<sup>12</sup>
PM6:IT-4F	285	0.830	22.60	64.80	12.20	<sup>13</sup>
PM6+PS:L8-BO	300	0.885	26.14	78.46	18.15	<sup>14</sup>
	500	0.876	25.86	70.66	16.00	
PNTz4T:PC <sub>71</sub> BM	290	0.708	19.40	73.40	10.10	<sup>15</sup>
PM6:eC9	300	0.820	27.70	71.30	16.20	<sup>16</sup>
PffBT4T-2OD:PC <sub>71</sub> BM	300	0.730	19.86	71.59	10.40	<sup>17</sup>
PM7:BTP-4F	300	0.821	27.60	54.10	12.20	<sup>18</sup>
PM7:BTP-4F:PC <sub>61</sub> BM	300	0.802	26.80	66.70	14.30	
PM7:BP-4F:MF1	300	0.882	23.06	71.62	14.57	<sup>19</sup>
PM6:Y6:BTP-M	300	0.855	26.87	62.06	14.23	<sup>20</sup>
BTR:NITI:PC <sub>71</sub> BM	300	0.940	19.50	73.83	13.63	<sup>21</sup>
PffBT4T-2OD:PC <sub>71</sub> BM	300	0.770	18.80	75.00	10.80	<sup>22</sup>
P2:IT-4F:BTP-4Cl	300	0.870	21.98	70.00	12.98	<sup>23</sup>
D18:Y6	300	0.844	26.13	69.10	15.24	<sup>24</sup>
D18:Y6:PC <sub>61</sub> BM	300	0.860	26.15	72.60	16.32	<sup>24</sup>
	350	0.861	26.82	70.10	16.19	
PTQ10:N <sub>3</sub> :PC <sub>71</sub> BM	300	0.850	26.80	74.00	16.80	<sup>25</sup>
PM6:PBB1-F:Y6-BO-4Cl	300	0.838	27.43	71.33	16.40	<sup>26</sup>
PM6:PBB1-F:eC9	300	0.836	27.71	72.69	16.84	<sup>26</sup>
PM6:2PACz/Y6-BO	300	0.816	27.60	72.90	16.40	<sup>27</sup>
PM6:L8-BO	300	0.863	26.49	70.34	16.08	<sup>28</sup>

PM6:Y7-BO:Y6-1O	300	0.847	26.96	72.73	16.61	<sup>29</sup>
PM6:L8-BO:TBr	300	0.900	26.50	74.50	17.80	<sup>30</sup>
PM6:Y6	300	0.840	25.99	67.97	14.91	<sup>31</sup>
PM6:eC9:L8-BO-F	300	0.836	28.36	73.00	17.31	<sup>32</sup>
	500	0.862	28.06	65.60	15.21	
PM6:L8-BO	300	0.871	26.56	71.57	16.56	<sup>33</sup>
	400	0.870	25.28	70.98	15.61	
	500	0.862	23.98	69.35	14.33	
PM6:L8-BO:DY-TF	300	0.884	27.8	74.18	18.23	<sup>33</sup>
	400	0.884	26.6	73.36	17.25	
	500	0.883	25.8	69.83	15.91	
PT2:TTPTTT-4F:IDIC	300	0.870	20.60	66.70	12.20	<sup>34</sup>
	400	0.860	21.50	65.30	12.40	
	500	0.860	22.00	61.40	11.60	
PT2:TTPTTT-4F	400	0.870	20.50	56.50	10.10	<sup>34</sup>
	500	0.870	20.80	53.50	9.70	
PM6:Y6:BTR-Cl	300	0.835	27.68	66.16	15.28	<sup>35</sup>
	500	0.826	23.83	56.63	11.15	
PBDFDFBO/ITIC-F	300	0.890	17.93	72.28	11.53	<sup>36</sup>
	600	0.910	16.81	71.13	10.88	
D18:eC9	300	0.838	27.35	74.10	17.00	<sup>37</sup>
	500	0.814	23.40	65.70	12.53	
D18:A4T-16	500	0.897	21.44	72.00	13.85	<sup>37</sup>
	800	0.888	19.87	68.30	12.05	
PM6:BTR-Cl:CH1007	303	0.795	29.00	66.70	15.40	<sup>38</sup>
PTQ10:m-THE:m-PEH	303	0.887	26.53	76.56	18.02	<sup>39</sup>
PBDB-T:PJ1	305	0.870	21.10	65.00	12.10	<sup>40</sup>

PM6:eC9:L8-BO:BTP-S10	305	0.867	28.35	71.30	17.55	<sup>41</sup>
Si25:IEICO-4F	320	0.700	26.87	70.15	13.20	<sup>42</sup>
Si25:Y14	320	0.782	24.92	74.69	14.55	<sup>43</sup>
	390	0.782	24.53	73.68	14.79	
	430	0.782	25.57	73.38	15.39	
	480	0.782	26.29	71.87	15.26	
PffBT4T-C <sub>9</sub> -C <sub>13</sub> :PC <sub>71</sub> BM	350	0.780	19.80	73.00	11.70	<sup>44</sup>
PTB7-Th:PC <sub>71</sub> BM:BTR	350	0.751	21.40	70.00	11.40	<sup>45</sup>
PM6:Y6:F1	350	0.842	27.53	69.50	16.11	
	480	0.834	27.08	67.43	15.23	<sup>46</sup>
z-2F:PC <sub>71</sub> BM	350	0.820	19.45	6.50	10.62	<sup>47</sup>
PM6:F-2Cl	350	0.866	19.73	58.00	10.00	<sup>48</sup>
	500	0.852	19.78	53.00	9.03	
	600	0.879	19.61	58.00	10.05	
J61:m-ITIC	360	0.833	19.04	49.63	8.34	<sup>49</sup>
PTQ10:IDTPC	400	0.913	17.90	61.30	10.00	<sup>50</sup>
PFBT4T-C <sub>5</sub> Si-25%:PC <sub>71</sub> BM	420	0.760	19.08	74.12	11.09	<sup>51</sup>
PBDB-TF:IDIC-C <sub>5</sub> Ph	470	0.921	20.15	70.12	13.01	<sup>52</sup>
PM7:MF2	500	0.953	19.20	54.90	10.04	<sup>53</sup>
PM6:BTP-4Cl	1000	0.834	27.30	53.10	12.10	<sup>54</sup>

**Table S8.** The detailed COS of the PM6:eC9:TDY- $\alpha$ -based blend films with different thicknesses.

Thickness (nm)	COS (%)
70	6.1±0.9
100	8.6±0.8
150	10.2±0.6
200	12.7±1.0
300	15.6±0.8
500	17.7±0.8
700	18.3±0.5
1000	18.6±0.9

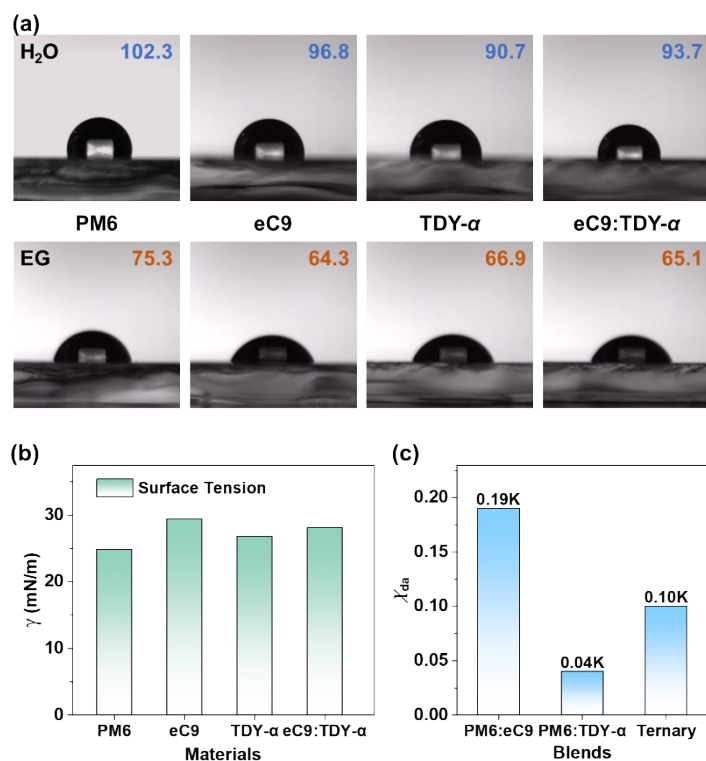


**Figure S11.** (a) The water and ethylene glycol contact angles of PM6, eC9 and TDY- $\alpha$  neat films and eC9:TDY- $\alpha$  (4:1) blend films. (b) The histogram of surface tension calculated from contact angles of PM6, eC9, TDY- $\alpha$  and eC9:TDY- $\alpha$  films. (c) The histogram of  $\chi_{da}$  values between donor and acceptors.

**Table S9.** Contact angle, surface tension and relative  $\chi_{da}$  values of PM6, eC9, TDY- $\alpha$  neat films and eC9:TDY- $\alpha$  blend films.

Films	Contact Angle (deg)		Surface Tension ( $\text{mN m}^{-1}$ )			$\chi_{da}$ with PM6
	Water	EG	$\gamma^d$	$\gamma^p$	$\gamma$	
PM6	104.2	75.3	2.98	21.86	24.85	/
eC9	96.1	63.7	5.33	24.08	29.41	0.19K
TDY	94.4	65.5	7.55	19.25	26.81	0.04K
eC9:TDY- $\alpha$	94.7	64.0	6.68	21.42	28.09	0.10K

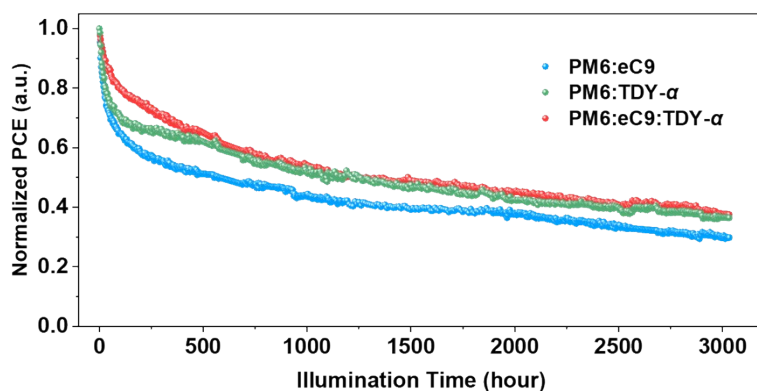


**Figure S12.** The evolution plots of normalized PCE for the PM6:eC9:TDY- $\alpha$ -based blend films with irradiation time under 1 sun illumination.

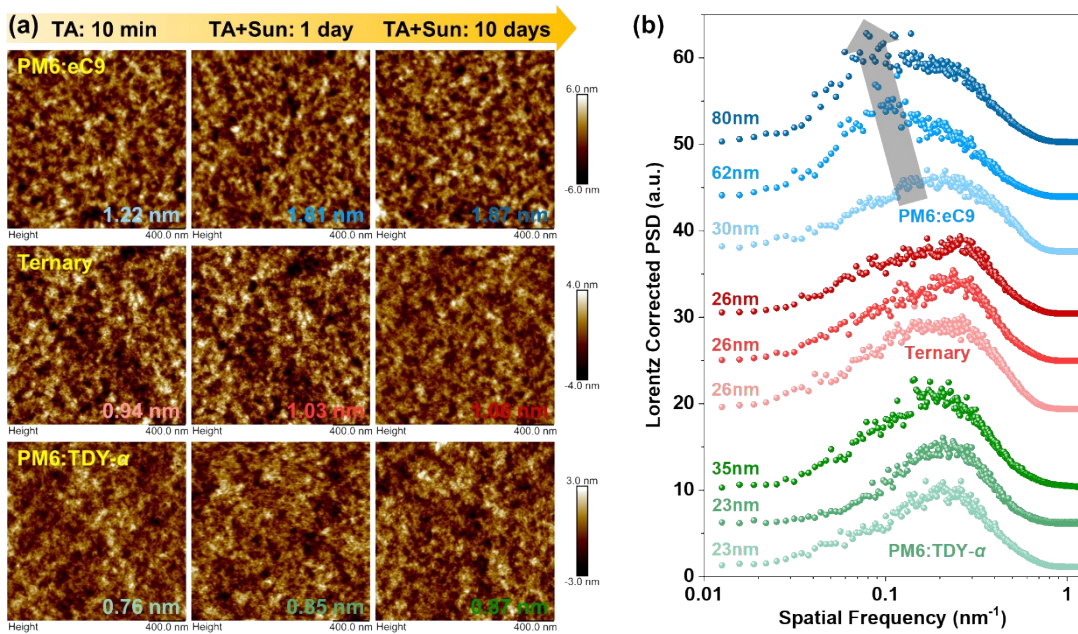


**Figure S13.** (a) The AFM height images of PM6:eC9, PM6:eC9:TDY- $\alpha$  and PM6:TDY- $\alpha$  blend films under 100 °C thermal stress and continuous light irradiation for 10 min, 1 day and 10 days. (b) Lorentz corrected PSD profiles of the phase images for the blend films.

**Table S10.** The peak positions and  $CL$  in OOP directions of PM6:eC9, PM6:eC9:TDY- $\alpha$  and PM6:TDY- $\alpha$  blend films with annealing for 10 min, 1 day and 10 days.

Sample	Time	Position ( $\text{\AA}^{-1}$ )	Stacking Distance ( $\text{\AA}$ )	FWHM ( $\text{\AA}^{-1}$ )	$CL$ ( $\text{\AA}$ )
PM6:eC9	10 min	1.77	3.54	0.26	21.45
	1 day	1.77	3.54	0.26	21.43
	10 days	1.78	3.53	0.25	22.30
Ternary	10 min	1.76	3.57	0.27	20.77
	1 day	1.76	3.58	0.27	21.23
	10 days	1.76	3.56	0.26	21.54
PM6:TDY- $\alpha$	10 min	1.76	3.56	0.27	21.05
	1 day	1.76	3.56	0.27	21.26
	10 days	1.77	3.55	0.26	21.81

**Table S11.** The peak positions and  $CL$  in IP directions of PM6:eC9, PM6:eC9:TDY- $\alpha$  and PM6:TDY- $\alpha$  blend films with annealing for 10 min, 1 day and 10 days.

Sample	Time	Position ( $\text{\AA}^{-1}$ )	Stacking Distance ( $\text{\AA}$ )	FWHM ( $\text{\AA}^{-1}$ )	$CL$ ( $\text{\AA}$ ) <sup>a</sup>
PM6:eC9	10 min	0.30	20.76	0.08	74.87
		0.39	15.91	0.09	66.01
	1 day	0.30	20.70	0.08	66.78
		0.40	15.72	0.08	69.00
	10 days	0.30	20.75	0.07	78.51
		0.40	15.88	0.07	85.27
Ternary	10 min	0.29	21.66	0.07	75.96
		0.38	16.65	0.11	53.78
	1 day	0.29	22.02	0.09	63.53
		0.38	16.36	0.13	43.13
	10 days	0.29	21.91	0.09	64.79
		0.38	16.33	0.12	45.76
PM6:TDY- $\alpha$	10 min	0.27	23.44	0.12	47.65
		0.41	15.29	0.19	29.60
	1 day	0.27	23.02	0.10	54.04
		0.39	15.93	0.22	25.53
	10 days	0.27	23.09	0.10	56.13
		0.40	15.56	0.21	27.29

<sup>a</sup> Coherence length ( $CL$ ) was calculated using the Scherrer equation of diffraction peaks:  $CL = 2\pi k/\Delta q$ , where  $k$  is the dimensionless shape factor (herein  $k = 0.9$ ) and  $\Delta q$  was the full width at half maximum (FWHM) of the given peak.

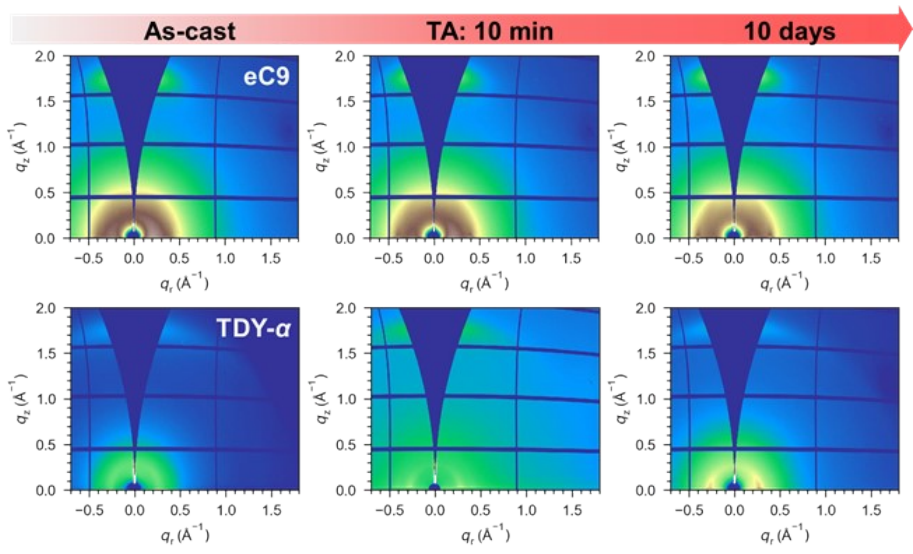


**Figure S14.** The 2D GIWAXS patterns of eC9 and TDY- $\alpha$  neat films under thermal stress for 0 s, 10 min and 10 days.

**Table S12.** The peak positions and *CL* in IP directions of eC9 and TDY- $\alpha$  neat films.

Sample	Time	Position ( $\text{\AA}^{-1}$ )	Stacking Distance ( $\text{\AA}$ )	FWHM ( $\text{\AA}^{-1}$ )	<i>CL</i> ( $\text{\AA}$ )
eC9	As-cast	0.28	22.55	0.25	22.62
		0.39	16.17	0.13	43.99
	10 min	0.28	22.34	0.25	23.00
		0.39	16.17	0.10	57.89
	10 days	0.30	21.25	0.24	23.36
		0.39	16.23	0.08	70.29
TDY- $\alpha$	As-cast	0.26	24.22	0.15	37.91
		0.39	16.05	0.21	27.04
	10 min	0.26	23.73	0.10	56.97
		0.39	16.12	0.20	27.75
	10 days	0.26	24.38	0.09	66.01
		0.39	16.24	0.24	23.56

**Table S13.** The peak positions and  $CL$  in OOP directions of eC9 and TDY- $\alpha$  neat films with annealing for 0 s, 10 min and 10 days.

Sample	Time	Position ( $\text{\AA}^{-1}$ )	Stacking Distance ( $\text{\AA}$ )	FWHM ( $\text{\AA}^{-1}$ )	$CL$ ( $\text{\AA}$ )
eC9	As-cast	1.74	3.61	0.33	17.34
	10 min	1.76	3.58	0.30	18.57
	10 days	1.77	3.56	0.29	19.33
TDY- $\alpha$	As-cast	1.76	3.57	0.31	18.21
	10 min	1.79	3.51	0.27	20.62
	10 days	1.79	3.51	0.23	24.67

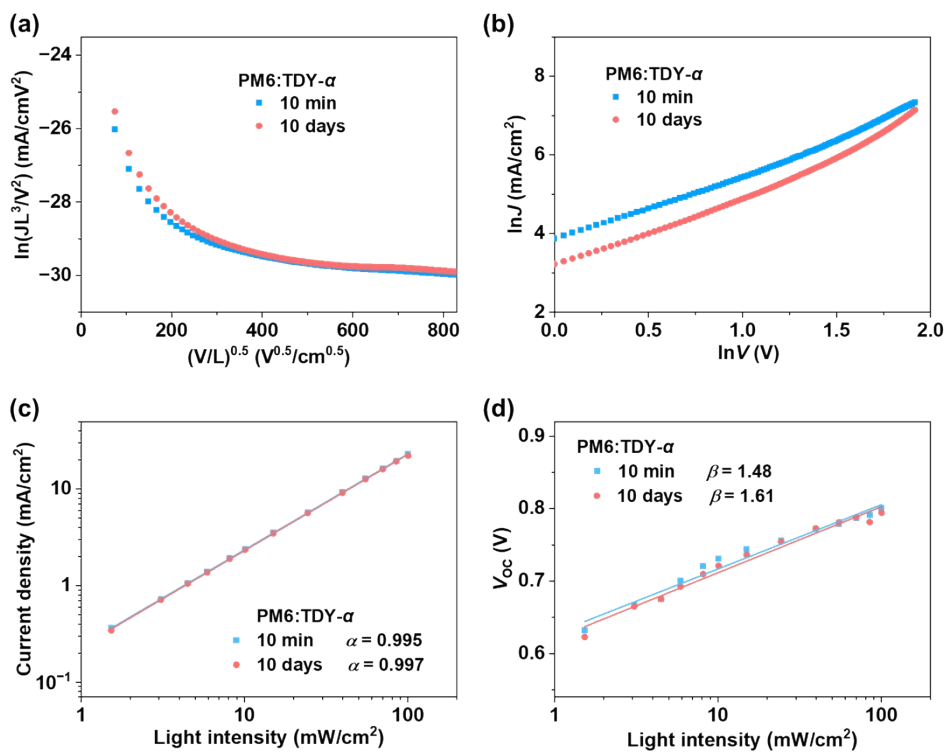


**Figure S15.** The (a) hole and (b) electron mobilities of PM6:TDY- $\alpha$ -based devices with different annealing time. The extracted plots of (a)  $J_{SC}$  and (b)  $V_{OC}$  versus light intensity for the devices.

**Table S14.** The detailed hole and electron mobilities parameters and  $\mu_h/\mu_e$  values of PM6:TDY- $\alpha$ -based devices with different annealing time.

Time	10 min	10 days
Hole ( $\text{cm}^2 \text{ V}^{-1} \text{ s}^{-1}$ )	7.25E-04	8.02E-04
Electron ( $\text{cm}^2 \text{ V}^{-1} \text{ s}^{-1}$ )	1.62E-04	8.42E-04
$\mu_h/\mu_e$	4.49	9.52

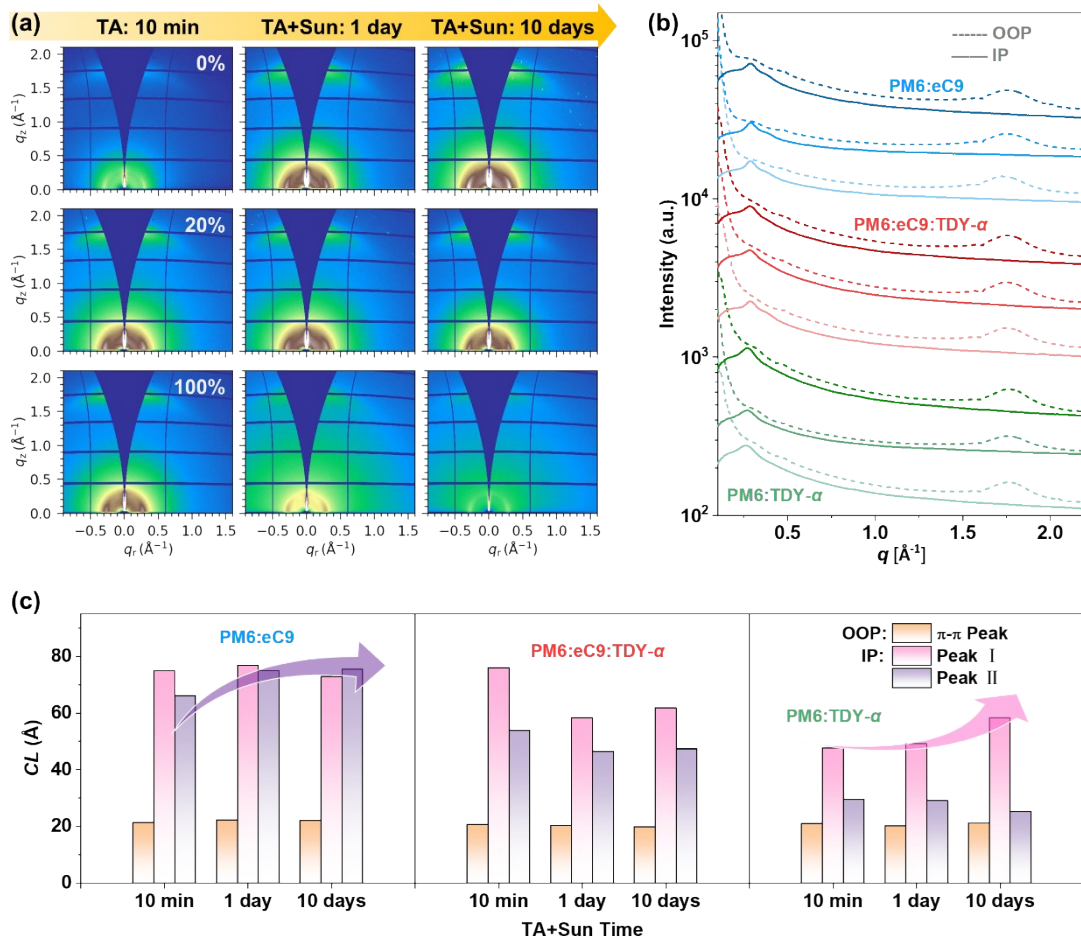


**Figure S16.** (a) The 2D GIWAXS patterns and (b) corresponding 1D line profiles of the blend films under 100 °C and continuous light irradiation. (c) The histogram of  $CL$  values.

**Table S15.** The peak positions and  $CL$  in IP directions of PM6:eC9, PM6:eC9:TDY- $\alpha$  and PM6:TDY- $\alpha$  blend films under 100 °C thermal stress and continuous light irradiation for 10 min, 1 day and 10 days.

Sample	Time	Position ( $\text{\AA}^{-1}$ )	Stacking Distance ( $\text{\AA}$ )	FWHM ( $\text{\AA}^{-1}$ )	$CL$ ( $\text{\AA}$ )
PM6:eC9	10 min	0.30	20.76	0.08	74.87
		0.39	15.91	0.09	66.01
	1 day	0.30	20.70	0.07	76.79
		0.40	15.89	0.08	74.81
		0.30	20.68	0.08	72.75
		0.40	15.80	0.07	75.43
	10 days	0.29	21.66	0.07	75.96
		0.38	16.65	0.11	53.78
Ternary	1 day	0.29	21.83	0.10	58.28
		0.39	16.30	0.12	46.50
		0.29	21.82	0.09	61.78
		0.38	16.42	0.12	47.38
	10 days	0.27	23.44	0.12	47.65
		0.41	15.29	0.19	29.60
		0.27	23.10	0.11	49.18
		0.40	15.54	0.19	29.20
PM6:TDY- $\alpha$	10 min	0.27	22.97	0.10	58.33
		0.39	16.03	0.22	25.24

**Table S16.** The peak positions and  $CL$  in OOP directions of the three blend films under 100 °C thermal stress and continuous light irradiation for 10 min, 1 day and 10 days.

Sample	Time	Position ( $\text{\AA}^{-1}$ )	Stacking Distance ( $\text{\AA}$ )	FWHM ( $\text{\AA}^{-1}$ )	$CL$ ( $\text{\AA}$ )
PM6:eC9	10 min	1.77	3.54	0.26	21.45
	1 day	1.77	3.55	0.25	22.38
	10 days	1.77	3.54	0.26	22.08
Ternary	10 min	1.76	3.57	0.27	20.77
	1 day	1.76	3.57	0.28	20.47
	10 days	1.76	3.57	0.28	19.94
PM6:TDY- $\alpha$	10 min	1.76	3.56	0.27	21.05
	1 day	1.76	3.57	0.28	20.29
	10 days	1.77	3.55	0.27	21.32

**Table S17.** Detailed photovoltaic parameters of PM6:eC9:TDY- $\alpha$ -based IS-OPV devices with different active layer thicknesses under the illumination of AM 1.5G. TPU was used as the substrate.

Thickness (nm)	$V_{OC}$ (V)	$J_{SC}$ ( $\text{mA cm}^{-2}$ )	FF (%)	PCE (%)
100	0.818	25.51	72.26	15.07
200	0.812	27.48	54.29	12.12
300	0.807	27.16	51.95	11.38
500	0.788	27.71	46.57	10.16
1000	0.790	23.26	40.10	7.37

**Table S18.** Detailed photovoltaic parameters of PM6:eC9:TDY- $\alpha$ -based devices during stretching under the illumination of AM 1.5G.

Strain (%)	$V_{OC}$ (V)	$J_{SC}$ (mA cm $^{-2}$ )	FF (%)	PCE (%)	Effective Area (mm)	Output Power (mW)
0	0.818	25.51	72.26	15.07	4.00	0.603
3	0.817	25.60	71.91	15.03	4.07	0.612
6	0.814	25.28	72.69	14.95	4.14	0.619
9	0.814	25.38	71.53	14.80	4.21	0.623
15	0.595	4.04	23.22	0.558	4.32	0.024

## References

- Y. Bai, Z. Zhang, Q. Zhou, H. Geng, Q. Chen, S. Kim, R. Zhang, C. Zhang, B. Chang, S. Li, H. Fu, L. Xue, H. Wang, W. Li, W. Chen, M. Gao, L. Ye, Y. Zhou, Y. Ouyang, C. Zhang, F. Gao, C. Yang, Y. Li and Z.-G. Zhang, *Nat. Commun.*, 2023, **14**, 2926.
- E.-Y. Shin, S. H. Park, Y. Jeon, K. Kim, G. Lee, J.-Y. Lee and H. J. Son, *Acs Appl Energ Mater*, 2023, **6**, 8729-8737.
- G. Sun, X. Jiang, X. Li, L. Meng, J. Zhang, S. Qin, X. Kong, J. Li, J. Xin, W. Ma and Y. Li, *Nat. Commun.*, 2022, **13**, 5267.
- H. Li, Y. Li, X. Dai, X. Xu and Q. Peng, *Angew. Chem. Int. Ed.*, 2024, e202416866.
- Y. Yu, J. Wang, Z. Chen, Y. Xiao, Z. Fu, T. Zhang, H. Yuan, X.-T. Hao, L. Ye, Y. Cui and J. Hou, *Sci. China Chem.*, 2024, **67**, 4194-4201.
- L. Zhu, M. Zhang, G. Zhou, Z. Wang, W. Zhong, J. Zhuang, Z. Zhou, X. Gao, L. Kan, B. Hao, F. Han, R. Zeng, X. Xue, S. Xu, H. Jing, B. Xiao, H. Zhu, Y. Zhang and F. Liu, *Joule*, 2024, **8**, 3153-3168.
- X. Guo, C. Cui, M. Zhang, L. Huo, Y. Huang, J. Hou and Y. Li, *Energy Environ. Sci.*, 2012, **5**, 7943-7949.
- H. Zhang, Y. Liu, G. Ran, H. Li, W. Zhang, P. Cheng and Z. Bo, *Adv. Mater.*, 2024, **36**, 2400521.
- S. C. Price, A. C. Stuart, L. Yang, H. Zhou and W. You, *J. Am. Chem. Soc.*, 2011, **133**, 4625-4631.
- M. Xiao, K. Zhang, Y. Jin, Q. Yin, W. Zhong, F. Huang and Y. Cao, *Nano Energy*, 2018, **48**, 53-62.
- Y. Jin, Z. Chen, M. Xiao, J. Peng, B. Fan, L. Ying, G. Zhang, X. F. Jiang, Q. Yin, Z. Liang, F. Huang and Y. Cao, *Adv. Energy Mater.*, 2017, **7**, 1700944.
- T. Wang, M.-S. Niu, Z.-C. Wen, Z.-N. Jiang, C.-C. Qin, X.-Y. Wang, H.-Y. Liu, X.-Y. Li, H. Yin, J.-Q. Liu and X.-T. Hao, *ACS Appl. Mater. Interfaces*, 2021, **13**, 11134-11143.

13. Q. Fan, W. Su, Y. Wang, B. Guo, Y. Jiang, X. Guo, F. Liu, T. P. Russell, M. Zhang and Y. Li, *Sci. China Chem.*, 2018, **61**, 531-537.
14. Z. Fu, J. W. Qiao, F. Z. Cui, W. Q. Zhang, L. H. Wang, P. Lu, H. Yin, X. Y. Du, W. Qin and X. T. Hao, *Adv. Mater.*, 2024, **36**, 2313532.
15. V. Vohra, K. Kawashima, T. Kakara, T. Koganezawa, I. Osaka, K. Takimiya and H. Murata, *Nat. Photon.*, 2015, **9**, 403-408.
16. W. Li, S. Zeiske, O. J. Sandberg, D. B. Riley, P. Meredith and A. Armin, *Energy Environ. Sci.*, 2021, **14**, 6484-6493.
17. X. Zhang, P. Fan, Z. Wang, D. Zheng and J. Yu, *J. Phys. Chem. C*, 2021, **125**, 15194-15199.
18. L. Ma, Y. Xu, Y. Zu, Q. Liao, B. Xu, C. An, S. Zhang and J. Hou, *Sci. China Chem.*, 2019, **63**, 21-27.
19. J. Gao, W. Gao, X. Ma, Z. Hu, C. Xu, X. Wang, Q. An, C. Yang, X. Zhang and F. Zhang, *Energy Environ. Sci.*, 2020, **13**, 958-967.
20. L. Zhan, S. Li, T.-K. Lau, Y. Cui, X. Lu, M. Shi, C.-Z. Li, H. Li, J. Hou and H. Chen, *Energy Environ. Sci.*, 2020, **13**, 635-645.
21. Z. Zhou, S. Xu, J. Song, Y. Jin, Q. Yue, Y. Qian, F. Liu, F. Zhang and X. Zhu, *Nat. Energy*, 2018, **3**, 952-959.
22. Y. Liu, J. Zhao, Z. Li, C. Mu, W. Ma, H. Hu, K. Jiang, H. Lin, H. Ade and H. Yan, *Nat. Commun.*, 2014, **5**, 5293.
23. T. Gokulnath, S. S. Reddy, H.-Y. Park, J. Kim, J. Kim, M. Song, J. Yoon and S.-H. Jin, *Solar RRL*, 2021, **5**, 2000787.
24. J. Qin, L. Zhang, Z. Xiao, S. Chen, K. Sun, Z. Zang, C. Yi, Y. Yuan, Z. Jin, F. Hao, Y. Cheng, Q. Bao and L. Ding, *Sci. Bull.*, 2020, **65**, 1979-1982.
25. C. H. Y. Ho, Y. Pei, Y. Qin, C. Zhang, Z. Peng, I. Angunawela, A. L. Jones, H. Yin, H. F. Iqbal, J. R. Reynolds, K. Gundogdu, H. Ade, S. K. So and F. So, *ACS Appl. Mater. Interfaces*, 2022, **14**, 47961-47970.
26. J. Wang, C. Han, J. Han, F. Bi, X. Sun, S. Wen, C. Yang, C. Yang, X. Bao and J. Chu, *Adv. Energy Mater.*, 2022, **12**, 2201614.
27. J. Jing, S. Dong, K. Zhang, Z. Zhou, J. Zhang, Q. Xue and F. Huang, *Solar RRL*, 2022, **6**, 2200682.
28. X. Zhang, C. Li, J. Xu, R. Wang, J. Song, H. Zhang, Y. Li, Y.-N. Jing, S. Li, G. Wu, J. Zhou, X. Li, Y. Zhang, X. Li, J. Zhang, C. Zhang, H. Zhou, Y. Sun and Y. Zhang, *Joule*, 2022, **6**, 444-457.
29. H. R. Bai, Q. An, M. Jiang, H. S. Ryu, J. Yang, X. J. Zhou, H. F. Zhi, C. Yang, X. Li, H. Y. Woo and J. L. Wang, *Adv. Funct. Mater.*, 2022, **32**, 2200807.
30. X. Song, H. Xu, X. Jiang, S. Gao, X. Zhou, S. Xu, J. Li, J. Yu, W. Liu, W. Zhu and P. Müller-Buschbaum, *Energy Environ. Sci.*, 2023, **16**, 3441-3452.
31. L. Zhang, S. Yang, B. Ning, F. Yang, W. Deng, Z. Xing, Z. Bi, K. Zhou, Y. Zhang, X. Hu, B. Yang, J. Yang, Y. Zou, W. Ma and Y. Yuan, *Solar RRL*, 2022, **6**, 2100838.
32. Y. Cai, Q. Li, G. Lu, H. S. Ryu, Y. Li, H. Jin, Z. Chen, Z. Tang, G. Lu, X. Hao, H. Y. Woo, C. Zhang and Y. Sun, *Nat. Commun.*, 2022, **13**, 2369.
33. Y. Wei, Y. Cai, X. Gu, G. Yao, Z. Fu, Y. Zhu, J. Yang, J. Dai, J. Zhang, X. Zhang, X. Hao, G. Lu, Z. Tang, Q. Peng, C. Zhang and H. Huang, *Adv. Mater.*, 2023, **36**, 2304225.

34. K. Weng, L. Ye, C. Li, Z. Shen, J. Xu, X. Feng, T. Xia, S. Tan, G. Lu, F. Liu and Y. Sun, *Solar RRL*, 2020, **4**, 2000476.
35. L. Zhang, L. Hu, X. Wang, H. Mao, L. Zeng, L. Tan, X. Zhuang and Y. Chen, *Adv. Funct. Mater.*, 2022, **32**, 2202103.
36. G. PanFeng, W. LiYong, F. HaiYan and D. Yuan, *Eur. Polym. J.*, 2022, **172**, 111189.
37. X. Xie, R. Ma, Y. Luo, T. A. Dela Peña, P. W. K. Fong, D. Luo, H. T. Chandran, T. Jia, M. Li, J. Wu, A. K. K. Kyaw and G. Li, *Adv. Energy Mater.*, 2024, **14**, 2401355.
38. H. Zhao, J. Xue, H. Wu, B. Lin, Y. Cai, K. Zhou, D. Yun, Z. Tang and W. Ma, *Adv. Funct. Mater.*, 2022, **33**, 2210534.
39. X. Kong, J. Zhang, L. Meng, C. Sun, X. Jiang, J. Zhang, C. Zhu, G. Sun, J. Li, X. Li, Z. Wei and Y. Li, *CCS Chem.*, 2023, **5**, 2945-2955.
40. T. Jia, J. Zhang, W. Zhong, Y. Liang, K. Zhang, S. Dong, L. Ying, F. Liu, X. Wang, F. Huang and Y. Cao, *Nano Energy*, 2020, **72**, 104718.
41. L. Zhan, S. Yin, Y. Li, S. Li, T. Chen, R. Sun, J. Min, G. Zhou, H. Zhu, Y. Chen, J. Fang, C. Q. Ma, X. Xia, X. Lu, H. Qiu, W. Fu and H. Chen, *Adv. Mater.*, 2022, **34**, 2206269.
42. Z. Wang, H. Jiang, X. Liu, J. Liang, L. Zhang, L. Qing, Q. Wang, W. Zhang, Y. Cao and J. Chen, *J. Mater. Chem. A*, 2020, **8**, 7765-7774.
43. F. Pan, M. Luo, X. Liu, H. Jiang, Z. Wang, D. Yuan, Q. Wang, L. Qing, Z. Zhang, L. Zhang, Y. Zou and J. Chen, *J. Mater. Chem. A*, 2021, **9**, 7129-7136.
44. J. Zhao, Y. Li, G. Yang, K. Jiang, H. Lin, H. Ade, W. Ma and H. Yan, *Nat. Energy*, 2016, **1**, 15027.
45. G. Zhang, K. Zhang, Q. Yin, X.-F. Jiang, Z. Wang, J. Xin, W. Ma, H. Yan, F. Huang and Y. Cao, *J. Am. Chem. Soc.*, 2017, **139**, 2387-2395.
46. F. Zhao, D. He, C. Zou, Y. Li, K. Wang, J. Zhang, S. Yang, Y. Tu, C. Wang and Y. Lin, *Adv. Mater.*, 2023, **35**, 2210463.
47. J. Lee, D. H. Sin, B. Moon, J. Shin, H. G. Kim, M. Kim and K. Cho, *Energy Environ. Sci.*, 2017, **10**, 247-257.
48. Y. Zhang, H. Feng, L. Meng, Y. Wang, M. Chang, S. Li, Z. Guo, C. Li, N. Zheng, Z. Xie, X. Wan and Y. Chen, *Adv. Energy Mater.*, 2019, **9**, 1902688.
49. Y. Yang, Z.-G. Zhang, H. Bin, S. Chen, L. Gao, L. Xue, C. Yang and Y. Li, *J. Am. Chem. Soc.*, 2016, **138**, 15011-15018.
50. Z. Luo, C. Sun, S. Chen, Z. G. Zhang, K. Wu, B. Qiu, C. Yang, Y. Li and C. Yang, *Adv. Energy Mater.*, 2018, **8**, 1800856.
51. X. Liu, L. Nian, K. Gao, L. Zhang, L. Qing, Z. Wang, L. Ying, Z. Xie, Y. Ma, Y. Cao, F. Liu and J. Chen, *J. Mater. Chem. A*, 2017, **5**, 17619-17631.
52. Y. Li, L. Yu, L. Chen, C. Han, H. Jiang, Z. Liu, N. Zheng, J. Wang, M. Sun, R. Yang and X. Bao, *Innovation*, 2021, **2**, 100090.
53. W. Gao, Q. An, M. Hao, R. Sun, J. Yuan, F. Zhang, W. Ma, J. Min and C. Yang, *Adv. Funct. Mater.*, 2020, **30**, 1908336.
54. L. Ma, S. Zhang, H. Yao, Y. Xu, J. Wang, Y. Zu and J. Hou, *ACS Appl. Mater. Interfaces*, 2020, **12**, 18777-18784.